

## Absorbing boundary conditions for molecular dynamics and multiscale modeling

S. Namilae,<sup>1</sup> D. M. Nicholson,<sup>1</sup> P. K. V. V. Nukala,<sup>1</sup> C. Y. Gao,<sup>2</sup> Y. N. Osetsky,<sup>1</sup> and D. J. Keffer<sup>2</sup>

<sup>1</sup>*Computer Science and Mathematics Division, Oak Ridge National Laboratory, Oak Ridge, Tennessee 37831-6164, USA*

<sup>2</sup>*Department of Chemical Engineering, University of Tennessee, Knoxville, Tennessee 37996, USA*

(Received 30 April 2007; revised manuscript received 8 August 2007; published 24 October 2007)

We present an application of differential equation based local absorbing boundary conditions to molecular dynamics. The absorbing boundary conditions result in the absorption of the majority of waves incident perpendicular to the bounding surface. We demonstrate that boundary conditions developed for the wave equation can be applied to molecular dynamics. Comparisons with damping material boundary conditions are discussed. The concept is extended to the formulation of an atomistic-continuum multiscale scheme with handshaking between the regions based on absorbing boundary conditions. The multiscale model is effective in minimizing spurious reflections at the interface.

DOI: [10.1103/PhysRevB.76.144111](https://doi.org/10.1103/PhysRevB.76.144111)

PACS number(s): 02.70.Ns, 46.15.-x, 46.40.-f

### I. INTRODUCTION

The atomic detail provided by molecular dynamics (MD) and other atomistic modeling methods is invaluable for understanding material behavior, especially at nanoscale. However, modeling of thermomechanical behavior of materials at realistic length and time scales is still beyond the purview of atomistic simulations as it would require billions of degree of freedom and time steps. Multiscale methods that link atomistic and continuum methodologies exhibit promise for solving large scale problems while simultaneously providing atomistic detail where it is needed. In addition, multiscale models enable better understanding of material behavior that inherently consists of physical phenomena occurring at different scales.

There are numerous atomistic-continuum multiscale methods in the literature. Popular among these are the handshaking method by Abraham and co-workers,<sup>1</sup> the quasicontinuum method by Tadmor and co-workers,<sup>2,3</sup> and coarse grained molecular dynamics by Rudd and Broughton.<sup>4</sup> Handshaking methods by Abraham and co-workers are based on specifying the overall Hamiltonian of the system as a combination of molecular dynamics, finite element, and handshake Hamiltonians to obtain the equations of motion. In quasicontinuum methods, the total energy of the system is calculated using interatomic potentials, while explicit atomic positions are calculated at fine scale; the coarse scale solution is calculated using the Cauchy-Born rule.<sup>2</sup> Coarse grained molecular dynamics techniques use a statistical coarse graining procedure at coarse scales and become equivalent to molecular dynamics at fine scales. Several other methods have been recently developed, e.g., Liu and Wagner's bridging scale method<sup>5</sup> uses a projection tensor to map atomistic displacements onto the continuum solution, so that the mean square difference of individual displacements is minimized. Shilkrot and co-workers<sup>6</sup> have coupled molecular dynamics with continuum dislocation dynamics.

Most of the above methods involve an atomistic method (usually molecular dynamics or statics) and a continuum formulation (usually finite element method) and a scheme to combine the two based on displacements or strains, forces or stresses, energies, or a combination thereof. The numerical

and physical differences between the atomistic and continuum methods lead to spurious reflections at the interface. A similar problem of wave reflection exists in the area of wave mechanics when an elastic, acoustic, or electromagnetic wave encounters a bounded region. This problem has been tackled using boundary conditions called absorbing boundary conditions (ABCs).<sup>7,8</sup> ABCs can be categorized as material based or differential equation based. Material based boundary conditions include the perfectly matched layer (PML) where a lossy or viscous material with complex coordinate stretching is added at the boundary to minimize reflections.<sup>9</sup> Differential equation based boundary conditions can be nonlocal; these strive for exact absorption by using Green's function and convolution operators on the entire domain<sup>10</sup> but they are difficult to implement and computationally prohibitive. Local absorbing boundary conditions are applied only on the boundary and are based on approximating the impedance of the unbounded exterior region. Engquist and Majda developed a series of boundaries of increasing accuracy based on this idea.<sup>11</sup> Multidirectional absorbers by Higdon<sup>12</sup> are a generalization of these boundary conditions. Recently higher order implementations of these boundary conditions have been developed by Guddati *et al.*<sup>13,14</sup> and Givoli.<sup>8,15</sup>

Several researchers have developed methods to minimize boundary reflections in atomistic-continuum multiscale models. Cai *et al.*<sup>16</sup> developed a nonlocal absorbing boundary condition based on a generalized Langevin equation and applied it to a one dimensional case. Karpov and co-workers<sup>17</sup> have expanded this to a general lattice in conjunction with the bridging scales multiscale method. E and co-workers<sup>18</sup> use local boundary conditions based on minimizing the reflection coefficient to address this problem. Qu and co-workers<sup>19</sup> use stadium boundary conditions developed earlier by Zhou *et al.*<sup>20</sup> that consist of adding an additional damping material to absorb the waves. Perfectly matched layers for the bridging scale approach developed by Li and To<sup>21</sup> are based on a similar idea. Yang *et al.*<sup>22</sup> have compared variational boundary conditions and damping material boundary conditions. In spite of these advances differential equation based boundary conditions like Engquist-Majda boundary conditions or higher order local ABCs have not

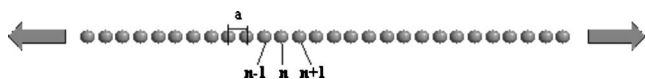


FIG. 1. Schematic of one dimensional chain of atoms.

been directly applied to molecular dynamics or multiscale modeling.

In this paper our objective is to demonstrate the applicability of Engquist-Majda type ABCs in molecular dynamics simulations. These are one dimensional boundary conditions based on impedance matching and have been effectively applied in finite element and finite difference schemes. In addition, they form the basis for several higher order ABCs.<sup>12-15,31</sup> We apply these ABCs to minimize wave reflections in molecular dynamics simulations. We further propose a multiscale model with molecular dynamics describing the atomistic regime and dynamic finite elements describing the continuum regime with information passing using ABCs.

## II. ABSORBING BOUNDARY CONDITIONS FOR MOLECULAR DYNAMICS SIMULATIONS

The problem of the boundary condition for molecular dynamics is very similar to the boundary condition for the wave equation. First, we consider the relationship between the discrete and continuum descriptions. It may be noted that the comparison between discrete lattice models and continuum models goes back to Born and Huang<sup>23</sup> who derived higher order elastic constants for a lattice with a given interatomic potential. Consider a system of atoms interacting based on an interatomic potential  $\Phi(r)$  where  $r$  is the distance between the particles. The equations of motion for a particle  $i$  located at  $\vec{r}_i$  surrounded by atoms  $j$  located at  $\vec{r}_j$  is given by Eqs. (1) and (2) below. Here  $\vec{r}_{ij}$  is the position vector given by  $\vec{r}_{ij} = \vec{r}_i - \vec{r}_j$ ,

$$\vec{F}_i = m \frac{d^2 \vec{r}_i}{dt^2} - \sum_j \vec{f}_{ij} + \vec{f}_i^{ext} \quad (1)$$

$$= m \frac{d^2 \vec{r}_i}{dt^2} - \sum_j \frac{d\Phi}{d\vec{r}_{ij}} + \vec{f}_i^{ext}, \quad (2)$$

i.e., the force experienced by particle  $i$  is sum of forces between the  $i$ - $j$  atom pairs (which in turn is given by interatomic potential) and any external force on the atom. Consider the one dimensional problem in Fig. 1 with the initial spacing  $a$  between the atoms. This one-dimensional lattice problem is similar to the Fermi-Pasta-Ulam problem and the Frenkel-Kontorova problem; both of these have been well studied as discrete lattice problems and also in relation to equivalent continuum descriptions.<sup>24-27</sup> Now, consider that the interaction of nearest neighbors along the one dimensional chain, ignoring the external force equation of motion for the  $n$ th particle, is

$$m \frac{d^2 r_n}{dt^2} = \frac{d\Phi}{dr_{n+1n}} - \frac{d\Phi}{dr_{nn-1}}. \quad (3)$$

Consider the normalized bond length of the  $n$ th bond given by  $u_n = \frac{r_{n+1} - r_n}{a}$ . Now, if we define a function  $T$  such that

$$T(u_n) = \frac{1}{a} \frac{d\Phi}{du_n}, \quad (4)$$

the equation of motion (3) becomes

$$m \frac{d^2 r_n}{dt^2} = T(u_{n+1}) - T(u_n) \quad (5)$$

in terms of  $u_n$ ,

$$ma \frac{d^2 u_n}{dt^2} = T(u_{n+1}) - 2T(u_n) + T(u_{n-1}). \quad (6)$$

Now we can divide by  $a^2$  and consider the continuum limit where  $a \rightarrow 0$ . This leads to a nonlinear wave equation of the form

$$\rho \frac{d^2 u}{dt^2} = \frac{d^2 T(u)}{dx^2}. \quad (7)$$

Here  $\rho$  is the mass density. When the interatomic potential is given by a harmonic function, for example, if  $\Phi = \frac{1}{2} \frac{k}{a} r^2$ , then  $T(u) = ku$  and Eq. (7) reduces to the linear wave equation. If the potential is a generic function, we can express Eq. (7) as

$$\rho \frac{d^2 u}{dt^2} = \frac{d}{dx} \left( k(u) \frac{du}{dx} \right) \quad (8)$$

which is the equilibrium equation for material with nonlinear constitutive properties. Alternately Eqs. (6) and (7) can be expanded as a Taylor series to obtain higher order terms that provide corrections for the discrete form.<sup>24</sup> There are several discussions in the literature where extensions to two and three dimensions and to an increased number of neighbors are considered.<sup>24-27</sup> The above analysis shows that an equivalence between discrete molecular dynamics and continuum descriptions exists provided that the displacement gradient is much less than 1 and the displacement is small compared to the nearest neighbors over the simulated time.

As discussed in the Introduction there are several schemes developed to address the problem of unwanted reflections for the wave equation. Based on the discussion in the preceding paragraphs, there is a clear correspondence between discrete molecular dynamics models and wave equation; hence we are justified in attempting to apply the methods developed for wave equation to molecular dynamics. Engquist and Majda used pseudodifferential operators to derive a series of boundary conditions of increasing order that eliminate (or reduce) the reflection of waves in a bounded region.<sup>11</sup> These ABCs have formed the basis for numerous higher order non-reflecting boundary conditions that have been devised subsequently. For an elastic wave, the simplest conditions for absorbing plane waves incident normal to a surface are

$$\left( \frac{d}{dt} - c_L \frac{d}{dz} \right) u_L,$$

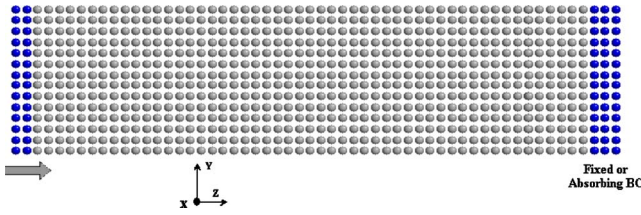


FIG. 2. (Color online) Schematic of the molecular dynamics setup.

$$\left( \frac{d}{dt} - c_T \frac{d}{dz} \right) u_T. \quad (9)$$

$c_L$  and  $c_T$  are the longitudinal and transverse elastic wave speeds in the material. Here,  $u_L$  and  $u_T$  are the displacements in longitudinal and transverse directions, while  $z$  is considered to be the longitudinal wave direction (see Fig. 2). We implement these boundary conditions in molecular dynamics simulations. Physically, the impedance of a semi-infinite region beyond the boundary is approximately matched by these ABCs. The ABC described in Eq. (9) is a simple but effective condition for absorbing the waves incident perpendicular to the boundary. In order to absorb waves in all directions and at corners one would require higher order ABCs, however, the focus here is to demonstrate the applicability of such ABCs to molecular dynamics and multiscale models, hence we use the simple form described in Eq. (9).

Figure 2 shows the typical molecular dynamics setup used. Two systems, the Lennard-Jones potential for fcc Al, and the Johnson potential<sup>28</sup> for bcc Fe, are studied. The Lennard-Jones potential is as shown below with parameters  $\sigma=2.551 \text{ \AA}$  and  $\varepsilon=0.408 \text{ eV}$  that are fit for fcc Al. We use a cutoff distance of  $5.6 \text{ \AA}$

$$U(r) = 4\varepsilon \left[ \left( \frac{\sigma}{r} \right)^{12} - \left( \frac{\sigma}{r} \right)^6 \right]. \quad (10)$$

The Johnson potential is in the form of a third degree polynomial with minima between the first and second neighbor distances in bcc iron. The Nordsieck predictor corrector algorithm is used for integration. The number of atoms for the different MD simulations varied between 5000 and 10 000 atoms. The methodology for implementing the ABCs discussed here is independent of the potential used; we have obtained results using both potentials. To demonstrate the independence from potential of the approach, the results presented in this section are based on the Lennard-Jones potential and those in the following section on multiscale modeling use the Johnson potential.

The molecular dynamics setup is three dimensional with periodic boundary conditions in the  $X$  and  $Y$  directions (see Fig. 2). A unidirectional wave is created in the system by rigidly displacing the atoms at one end of the bar. In one case atoms at the other end are fixed. This results in complete reflection of the wave and provides a mark for comparison. In the second case absorbing boundary conditions are applied. This is achieved by readjusting the evolution of atomic positions in the last three atomic layers according to Eq. (9).

The velocity of atoms in these layers is obtained as a function of the displacement gradient in the preceding layers multiplied by a factor  $c$ . The numerical value of  $c$  roughly corresponds to the wave speed, however, we obtain the value by optimizing the simulation such that there is minimal reflection at the boundary. We find that a value of  $0.05 \text{ \AA/fs}$  is optimal in reducing the reflections. This is of the same order as longitudinal wave speed in iron based on continuum calculations. In order to calculate the displacement gradient we use a backward difference scheme and compute the gradient as an average over five atomic layers preceding the boundary. One could use an alternate method to obtain the displacement gradient and the ABC would still be effective.

Figure 3 shows the contour plot of displacement experienced by atoms at various times as the planar wave travels toward the boundary. Figure 3(a) corresponds to the fixed boundary while Fig. 3(b) corresponds to the case when ABCs are applied at the boundary. It can be observed that when fixed boundary conditions are applied there is a complete reflection of the wave back into the domain. When ABCs are applied at the boundary the wave is completely absorbed as in Fig. 3(b).

It may be noted that the ABCs can absorb all the waves incident normal to the boundary. They can be effectively used for situations where the predominant direction of waves is normal to the boundary, even if some waves in other directions are present. Figure 4 shows the contour plots of displacement when the initial displacements are applied at varying rates resulting in a nonplanar wave front. Though some waves in other directions are present the predominant direction of wave motion is in the  $Z$  direction. It can be observed that the ABCs are effective in absorbing most of the waves.

Another example of application of the ABC is shown in Fig. 4.  $Z$  displacement contours of elastic waves generated due to displacement applied on a crack are shown in Fig. 5. The crack is opened by applying a small fixed displacement in the  $Y$  direction similar to crack tip opening displacement as shown in Fig. 5(a). Absorbing boundary conditions are applied at the three boundaries as shown. Note that the displacement wave in the  $Z$  direction would be longitudinal for the ABC along the  $Y$  axis and transverse for the two boundaries parallel to the  $Z$  axis. Figures 5(a)–5(e) show the displacement contours when ABCs are applied. These are compared to the case when fixed boundary conditions are applied in the place of ABCs in Figs. 5(f)–5(i). It can be observed that ABCs are effective in minimizing the reflections. Higher order ABCs are required for better absorption at corners and for waves incident at angles, however, current results demonstrate that simple ABCs can be effectively used in molecular dynamics simulations.

We now compare the local ABCs discussed above with material based ABCs. Material based ABCs consist of adding a lossy or viscous material which absorbs the waves from the domain with minimal reflections. Effectively the equations of motion in the damping region are modified by the addition of a damping or wave filtering term, while the equations of motion in the molecular dynamics region are unmodified. Stadium boundary conditions<sup>19,20</sup> and To and Li's<sup>21</sup> MD implementation of Berenger's perfectly matched layers<sup>9</sup> are

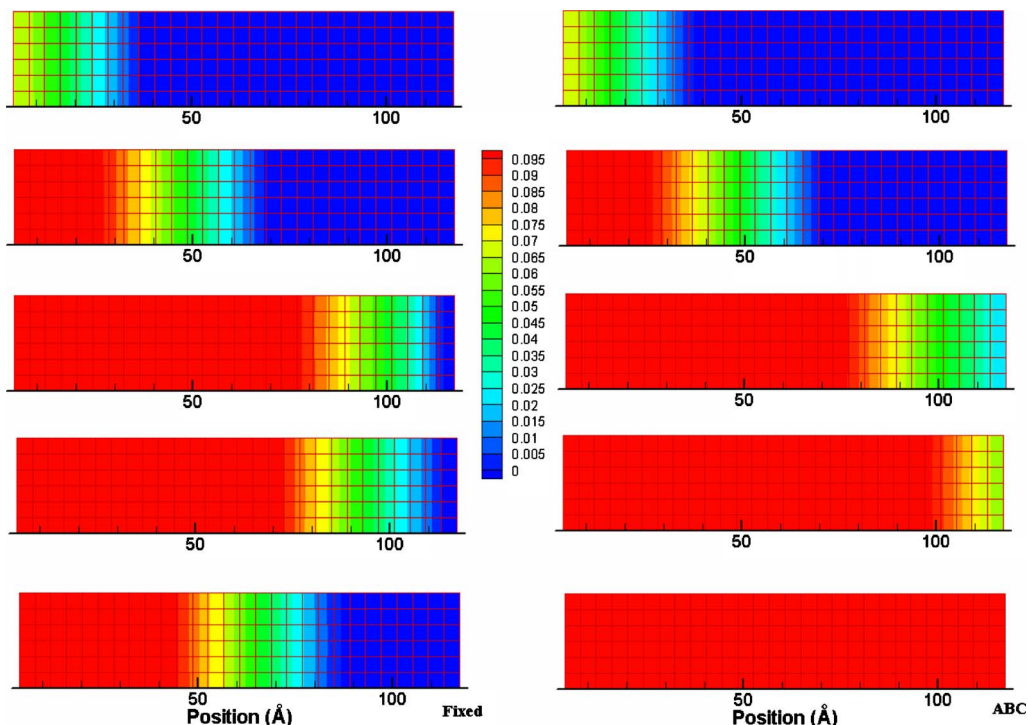


FIG. 3. (Color online) Displacement contour plots of wave motion (a) for fixed boundary showing the reflection (b) with ABCs. Plots correspond to 1, 1.7, 2.8, 3.2, and 4.2 ps, respectively. Position and displacement are in angstroms.

examples of this approach. For the simple case of adding viscous material, the modified equation of motion in the damping region is

$$m\ddot{\mathbf{r}}_i = \sum_j \vec{f}_{ij} + \vec{f}_{ij}^{ext} + d(z_i)\dot{\mathbf{r}}_i. \quad (11)$$

$d(z_i)$  is a damping function dependent on the position of the atom. It becomes equal to zero in the MD region and slowly ramps up the viscosity in the damping region. We find that the choice of  $d(z_i)$  is important for effective implementation; the gradual increase in viscosity into the damping region is necessary to avoid reflections. In the current case we use the cubic polynomial in Eq. (12) below as the damping function but any other function that would gradually increase the viscosity could be used:

$$d(z_i) = \eta_o \left[ \frac{z_i - d_1}{d_2 - d_1} \right]^3. \quad (12)$$

Here, the viscous material starts at  $d_1$  and ends at  $d_2$ ,  $z_i$  gives the position of the atom,  $\eta_o$  is the same parameter used in the Langevin thermostat and is dependent on the Debye frequency of the material. Due to the high viscosity, all the waves including low frequency modes that enter the damping region are absorbed. Figure 6 shows the contour plots of displacement for this boundary condition. It can be observed that damping material effectively absorbs the waves without reflection into the molecular dynamics region.

Among local ABCs and material ABCs there are advantages and disadvantages for both approaches. The obvious advantage of damping material ABCs is the ease of imple-

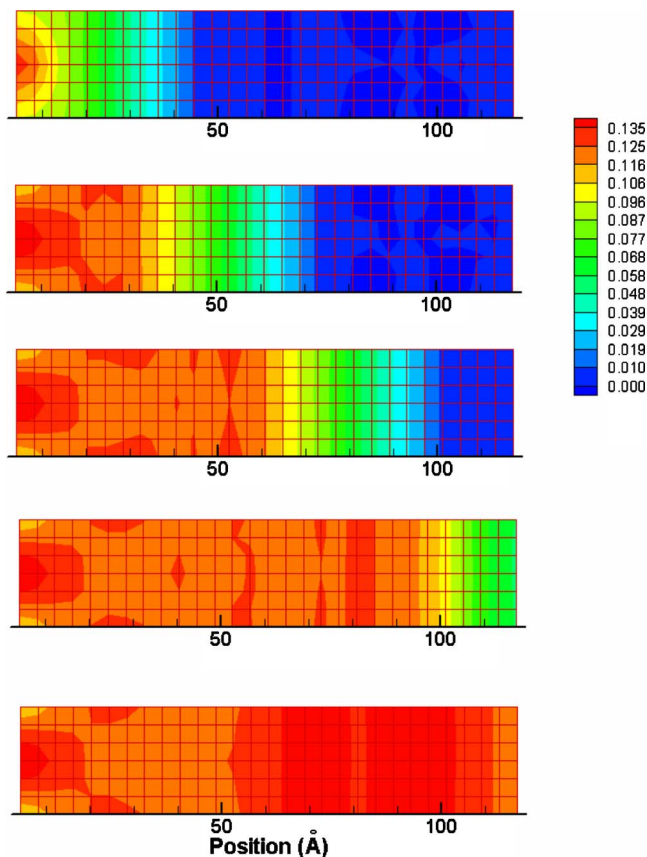


FIG. 4. (Color online) Contour plot for nonplanar wave front with ABCs. Plots correspond to 1.2, 1.8, 2.4, 3.0, and 3.6 ps, respectively.

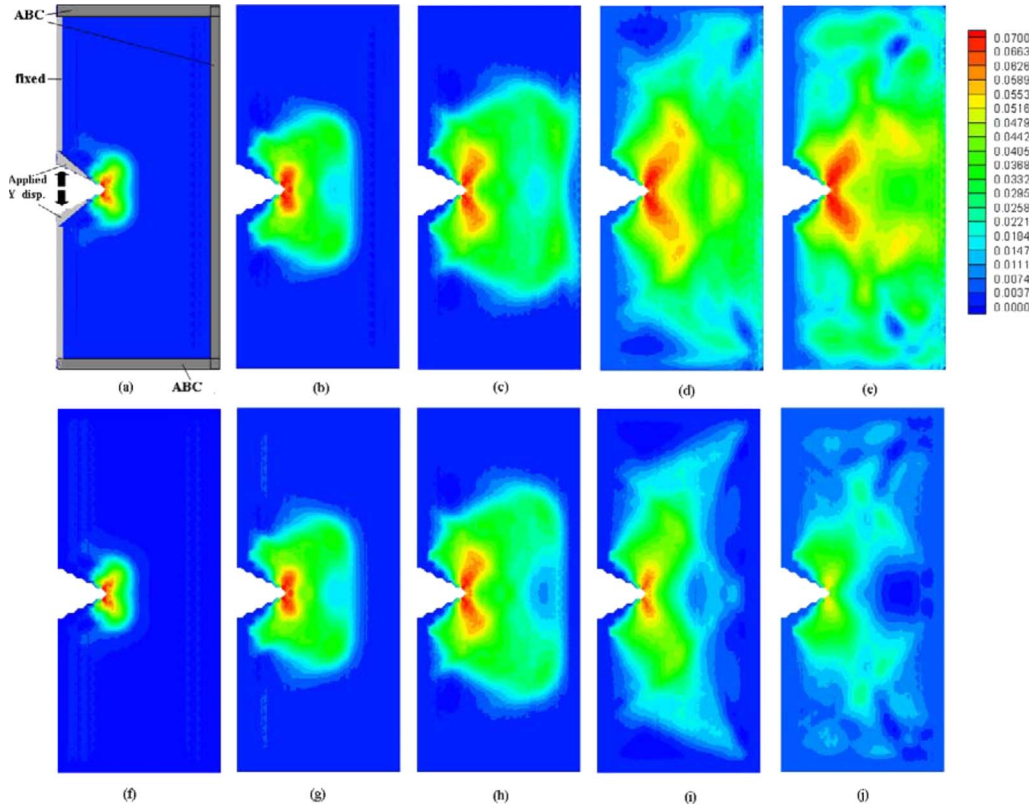


FIG. 5. (Color online) Contour plots of  $z$  displacement for crack opening. Displacement is applied on atoms near the crack as shown. Plots (a)–(e) show contours with absorbing boundary conditions at  $t=0.3, 0.6, 1, 1.6,$  and  $2$  ps. Plots (f)–(j) show similar displacement contours with fixed boundaries.

mentation. Second, it can absorb the waves entering from different directions. One disadvantage is that additional computation is required. For example, in the case studied here we had to use almost the same number of atoms in the damping material and the MD regions to damp out all the waves. One could optimize the damping function to reduce the size of the damping region, however, the computation is expected to be much larger than the MD region alone. Yang and co-workers<sup>22</sup> also demonstrate this point. A more significant disadvantage in the context of multiscale modeling is that waves would not pass on to the larger scale region if the MD and continuum are modeled independently and information (forces displacements and energies) passing occurs in an interface region. In the following section we develop a multiscale model with the interfacial region between MD and continuum based on the ABCs resulting in seamless wave propagation between the domains while simultaneously eliminating the reflections into the molecular dynamics domain.

### III. MULTISCALE MODEL

Consider an elastic material in domain  $\Omega$  subject to some external traction or displacement boundary conditions. We divide the region  $\Omega$  into two subdomains  $\Omega_1$  and  $\Omega_2$  with an interface  $\Gamma$  separating the two regions. The objective here is to develop a multiscale model with atomistic and continuum

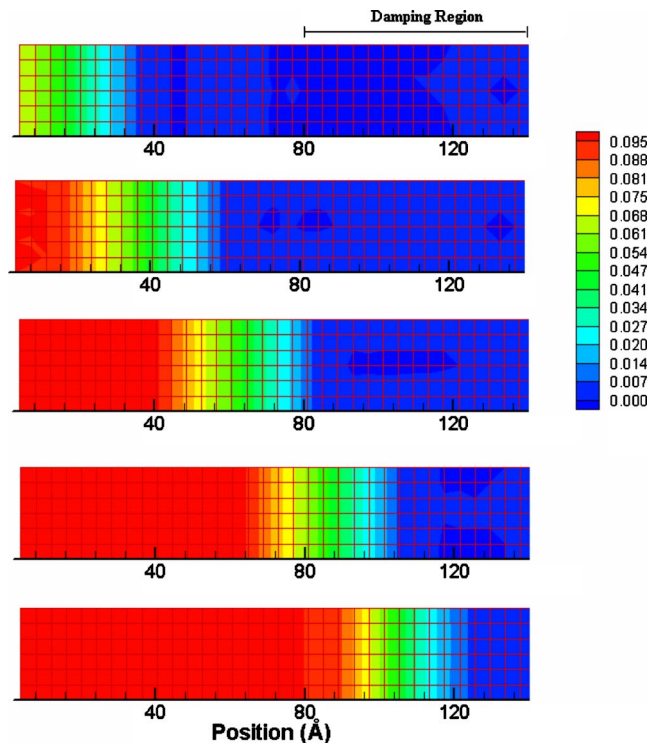


FIG. 6. (Color online) Displacement contours for damping material ABCs. Plots correspond to 1, 1.5, 2, 2.5, and 3 ps, respectively.

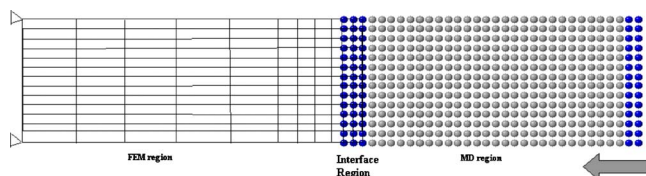


FIG. 7. (Color online) Schematic of multiscale modeling setup.

descriptions for the regions  $\Omega_1$  and  $\Omega_2$ , respectively, such that the elastic waves generated in region  $\Omega_1$  are passed onto region  $\Omega_2$  without any reflection at the interface  $\Gamma$ .

The domain  $\Omega_1$  is considered to be composed of atoms interacting through an interatomic potential. Newton's equations of motion for the three dimensional atomistic system are written as

$$\vec{F}_i = m \frac{d^2 \vec{u}_i}{dt^2} = \sum f_{ij} + \vec{f}_i^{ext}. \quad (13)$$

These equations are solved in a molecular dynamics formulation. The velocities and positions of the particles are obtained by numerical integration of the interatomic forces obtained by the potential.

The region  $\Omega_2$  is considered to be continuum and the dynamic equilibrium equation for this region is

$$m \ddot{\vec{u}} = \frac{d}{d\vec{r}} \left( k \frac{d\vec{u}}{d\vec{r}} \right) + \vec{f}^{ext}. \quad (14)$$

This equation is solved in a variational form using the finite element method.  $k$  here represents the elastic constants of the material. Different approaches can be used for time integration involved in the dynamics. In the present case we obtain the displacements, velocities, and accelerations using the Newmark direct integration algorithm.<sup>29</sup> Consider the matrix form of dynamic equilibrium equation at time  $t$ , the effective load vector  $\vec{F}_t$  at time  $t$  is obtained as

$$\vec{F}_t = K \cdot \vec{u}_{t-\Delta t} + C \cdot \dot{\vec{u}}_{t-\Delta t} + M \ddot{\vec{u}}_{t-\Delta t}. \quad (15)$$

Here  $K$  is the stiffness matrix,  $M$  is the mass matrix, and  $C$  is the so called damping matrix. The Newmark algorithm is a direct integration scheme to solve Eq. (15). In this approach, we obtain the effective stiffness matrix  $\bar{K}$  using static stiffness matrix  $K$ , mass matrix  $M$ , and damping matrix  $C$  as shown in Eq. (16). Here,  $\beta$  and  $\gamma$  are integration parameters,

$$\begin{aligned} \bar{K} &= K + b_1 C + b_2 M, \\ b_1 &= \frac{1}{\beta \Delta t^2}, \quad b_2 = \gamma \Delta t b_1. \end{aligned} \quad (16)$$

The effective load vector  $\vec{F}_t$  can be obtained from Eq. (15) expressing it in a form similar to Eq. (16). The equations are solved for displacement as

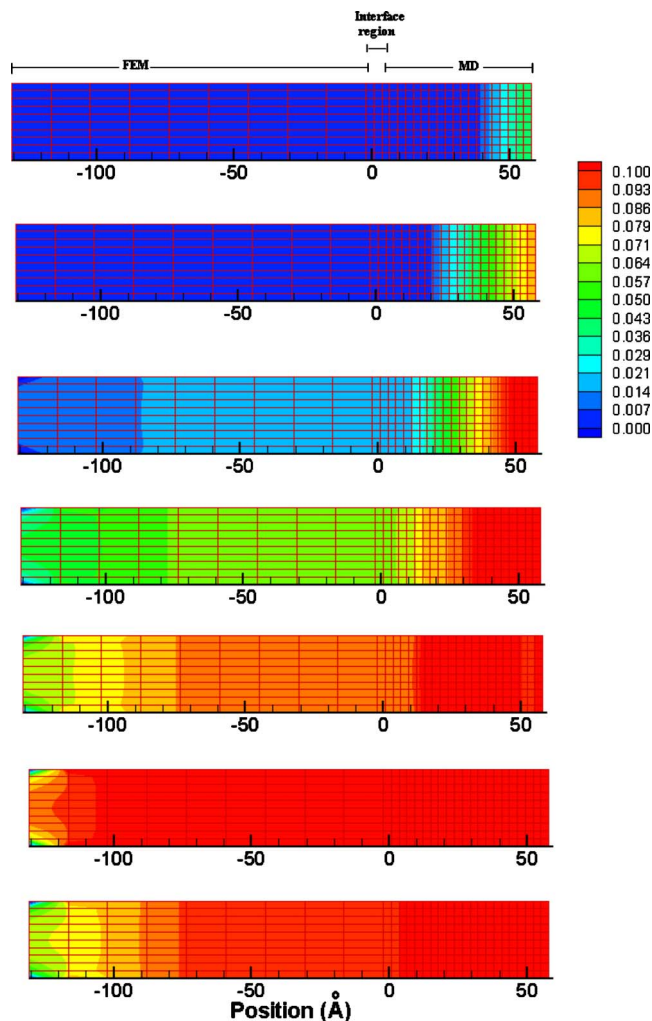


FIG. 8. (Color online) Displacement contours at increasing times (0.4, 0.7, 1.1, 1.4, 1.9, 2.1, and 2.4 ps). Plots show passage of waves from MD to finite element regime with minimal reflections.

$$\vec{u}_t = K^{-1} \vec{F}_t. \quad (17)$$

The velocities and accelerations at time  $t$  ( $\dot{\vec{u}}_t, \ddot{\vec{u}}_t$ ) are then calculated as functions of displacements at the current time step and the accelerations, velocities, and displacements in the previous time step ( $\vec{u}_{t-\Delta t}, \dot{\vec{u}}_{t-\Delta t}, \ddot{\vec{u}}_{t-\Delta t}$ ).

For coupling the two descriptions based on the molecular dynamics and finite element methods we use handshaking based on ABCs at the interface region  $\Gamma$ . The interface region is an overlap between the finite element and molecular dynamics region and consists of both nodes and pseudoatoms. Pseudoatoms are the atoms in the overlap region between continuum and discrete domains; they contribute to the forces on regular atoms but do not follow the molecular dynamics equations of motion. The velocities of the atoms in the interfacial region are obtained using Eq. (9) and are based on the displacement gradient in the preceding atomic planes. These velocities are passed on to the corresponding nodes in the interface region of the finite element method, i.e., the velocities of nodes in the interfacial region are ob-

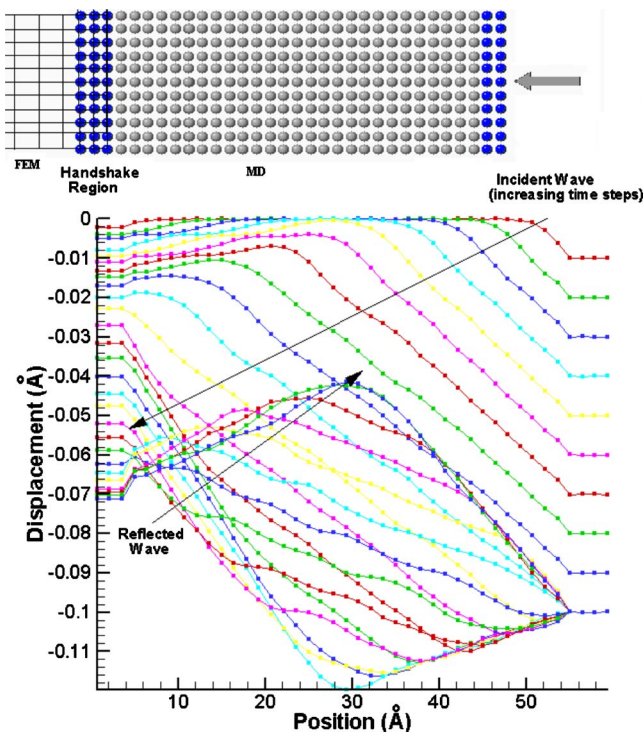


FIG. 9. (Color online) Schematic of displacement profile for MD region of multiscale model with regular handshaking.

tained using ABCs and not by the Newmark algorithm. The nodal displacements obtained from the finite element solution are passed on to the molecular dynamics simulations as the displacements of the pseudoatoms thus forming the two way coupling. Using this scheme, we find that elastic waves generated in the molecular dynamics regime are passed on to the finite element method with minimal reflections at the numerical interface between the regimes.

Figure 7 shows the schematic of the setup for the multiscale model. It consists of a three dimensional molecular dynamics region and a finite element region with an overlapped interface region. The atomistic part is composed of bcc iron atoms interacting with the Johnson potential.<sup>28</sup> We use the finite element method code NIKE3D for continuum simulations.<sup>30</sup> The constitutive response of the finite element region is single-crystal-elastic (orthotropic) with the elastic constants the same as those of the Johnson potential.<sup>28</sup> The multiscale simulations consist of 5782 atoms, 726 nodes, and 500 elements. There are 363 pseudoatoms and 242 nodes in the handshake region. An atomic unit cell in the handshake region corresponds to an element with an overlapping between nodes and atoms at the corners of the unit cell. The contribution of atoms at the center of the unit cell is distributed between the nodes corresponding to corners of the unit cell. A one dimensional wave is generated by rigidly displacing the atoms at one end of the atomistic region and ABCs are applied at the interface region.

Figure 8 shows the displacement contours of atoms and nodes in the multiscale model. It can be clearly noticed that the elastic wave generated in the molecular dynamics regime is passed on to the finite element regime with minimal re-

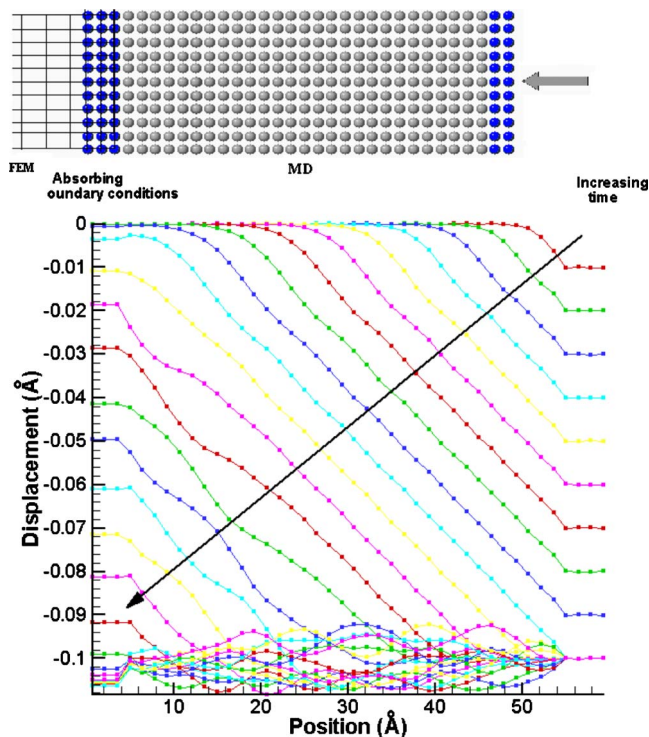


FIG. 10. (Color online) Schematic of displacement profile for MD region of multiscale model with ABCs. Reflections are minimal compared to regular handshaking in Fig. 8.

lections at the interface. It should be noted that the wave reflections are considerably reduced by using ABC based handshaking when compared to conventional handshaking based on forces and displacements. In the conventional handshaking algorithm, a region of overlap between atomistic and continuum domains exists as discussed earlier, in this region molecular dynamics passes atomic forces as nodal forces to the finite element regime, which in turn provides displacements of atoms back. This approach is based on an overall Hamiltonian.<sup>1</sup> Figure 9 shows the displacement profiles of atomic layers in the MD region at various times when this conventional handshaking is used. This can be compared with the similar displacement profiles in Fig. 10 when ABCs are used. It is clear that the reflections at the interface are minimal with ABCs.

We demonstrate that the differential equation based ABCs developed for wave equations can be applied to molecular dynamics and multiscale simulations. One of the major outstanding problems in continuum-atomistic multiscale models is the reflection of waves at the numerical interface. This is a problem in most existing multiscale methodologies including handshaking methods,<sup>1</sup> the quasicontinuum method,<sup>2</sup> and the bridging scale method.<sup>5</sup> There have been various attempts within these schemes but none have applied the generalization of continuum ABCs to discrete atomistic systems. Our approach is a simple but effective numerical scheme based on Engquist-Majda ABCs to address this issue. It may be noted that problems considered in this paper are three dimensional, however, the implementation of ABCs is strictly valid only for one dimensional longitudinal and transverse waves

incident perpendicular to the boundary. Higher order ABCs are required to address problems involving corners and waves incident at an angle to the boundary in an effective manner. Several implementations of such higher order ABCs are available in the literature.<sup>8,13-15</sup> Current results can possibly be extended to higher order approaches, for example, Givoli and co-workers' method of simplifying Higdon's multidirectional absorbers.<sup>12</sup> Higdon's boundary condition of order  $J$  is

$$\prod_j \left( \frac{d}{dt} - C_j \frac{d}{dx} \right) u = 0. \quad (18)$$

$C_j$  are parameters which signify directions or phase speeds of waves. While these boundary conditions are very general, application beyond  $J=3$  has been difficult because of higher order derivatives. Givoli and co-workers<sup>15,31</sup> recently developed a numerical scheme based on finite differences to apply these boundary conditions to arbitrary higher order. This approach can be adapted to molecular dynamics and multiscale modeling and is a part of future work.

#### IV. SUMMARY

We demonstrate the applicability of differential equation based absorbing boundary conditions to molecular dynamics simulations. The results are compared with damping material boundary conditions. A multiscale model is developed with the absorbing boundary conditions facilitating the passage of elastic waves from atomistic to finite element regions with minimal reflections at the interface.

#### ACKNOWLEDGMENTS

Support for C.Y.G. was provided by the University of Tennessee Computational Sciences Initiative. This research was sponsored by the Laboratory Directed Research and Development Program of Oak Ridge National Laboratory (ORNL), managed by UT-Battelle, LLC for the U.S. Department of Energy under Contract No. DE-AC05-00OR22725 and by the Division of Materials Sciences and Engineering, Office of Basic Energy Sciences, U.S. Department of Energy. We thank Yanfei Gao and Gorti Sarma for reviewing the manuscript.

- 
- <sup>1</sup>F. Abraham, J. Broughton, N. Bernstien, and E. Kaxarias, *Comput. Sci. Eng.* **12**, 538 (2001).  
<sup>2</sup>E. B. Tadmor, R. Phillips, and M. Ortiz, *Philos. Mag. A* **73**, 1529 (1996).  
<sup>3</sup>V. B. Shenoy, R. Miller, E. B. Tadmor, D. Rodney, R. Phillips, and M. Ortiz, *J. Mech. Phys. Solids* **47**, 611 (1999).  
<sup>4</sup>R. E. Rudd and J. Q. Broughton, *Phys. Status Solidi B* **217**, 251 (2000).  
<sup>5</sup>G. J. Wagner and W. K. Liu, *J. Comput. Phys.* **190**, 249 (2003).  
<sup>6</sup>L. E. Shilkrot, R. E. Miller, and W. A. Curtin, *J. Mech. Phys. Solids* **52**, 755 (2004).  
<sup>7</sup>D. Givoli, *J. Comput. Phys.* **94**, 1 (1991).  
<sup>8</sup>D. Givoli, *Wave Motion* **39**, 219 (2004).  
<sup>9</sup>J. P. Berenger, *J. Comput. Phys.* **114**, 185 (1994).  
<sup>10</sup>J. B. Keller and D. Givoli, *J. Comput. Phys.* **82**, 172 (1989).  
<sup>11</sup>B. Engquist and A. Majda, *Commun. Pure Appl. Math.* **32**, 313 (1979).  
<sup>12</sup>R. L. Higdon, *Math. Comput.* **49**, 65 (1987).  
<sup>13</sup>M. N. Guddati and J. L. Tassoulas, *J. Comput. Acoust.* **8**, 139 (2000).  
<sup>14</sup>M. N. Guddati and K. W. Lim, *Int. J. Numer. Methods Eng.* **66**, 949 (2006).  
<sup>15</sup>D. Givoli and B. Neta, *J. Comput. Phys.* **186**, 24 (2003).  
<sup>16</sup>W. Cai, M. de Koning, V. V. Bulatov, and S. Yip, *Phys. Rev. Lett.* **85**, 3213 (2000).  
<sup>17</sup>E. G. Karpov, G. J. Wagner, and W. K. Liu, *Int. J. Numer. Methods Eng.* **62**, 1250 (2005).  
<sup>18</sup>W. E and Z. Huang, *Phys. Rev. Lett.* **87**, 135501 (2001).  
<sup>19</sup>S. Qu, V. Shastry, W. A. Curtin, and R. E. Miller, *Modell. Simul. Mater. Sci. Eng.* **13**, 1101 (2005).  
<sup>20</sup>S. J. Zhou, P. S. Lomdahl, R. Thomson, and B. L. Holian, *Phys. Rev. Lett.* **76**, 2318 (1996).  
<sup>21</sup>A. C. To and S. Li, *Phys. Rev. B* **72**, 035414 (2005).  
<sup>22</sup>J. Z. Yang and X. Li, *Phys. Rev. B* **73**, 224111 (2006).  
<sup>23</sup>M. Born and K. Huang, *Dynamical Theory of Crystal Lattices* (Oxford University Press, London, 1954).  
<sup>24</sup>M. A. Collins, *Chem. Phys. Lett.* **77**, 342 (1981).  
<sup>25</sup>G. Friesecke and R. L. Pego, *Nonlinearity* **12**, 1601 (1999).  
<sup>26</sup>J. H. Batteb and J. D. Powell, *Phys. Rev. B* **20**, 1398 (1979).  
<sup>27</sup>V. A. Tarasov, *J. Math. Phys.* **47**, 092901 (2006).  
<sup>28</sup>R. A. Johnson, *Phys. Rev.* **134**, A1329 (1964).  
<sup>29</sup>N. M. Newmark, *J. Engrg. Mech. Div.* **85**, 67 (1959).  
<sup>30</sup>B. N. Maker, R. M. Ferencz, and J. O. Hallquist, Report No. UCRL-MA-105268, Lawrence Livermore National Laboratory, 1991.  
<sup>31</sup>V. J. van Joolen, B. Neta, and D. Givoli, *Int. J. Numer. Methods Eng.* **63**, 1041 (2005).